Frequency domain characterization of torque in tumbling ball mills using DEM modelling: Application to filling level monitoring

Francisco Pedrayes [a], Joaquín G. Norniella [a], Manuel G. Melero [a],*,
Juan M. Menéndez-Aguado [b], Juan J. del Coz-Díaz [c]

[a] Departamento de Ingeniería Eléctrica, Electrónica, de Computadores y Sistemas, Universidad de Oviedo, Spain
[b] Departamento de Explotación y Prospección de Minas, Universidad de Oviedo, Spain
[c] Departamento de Construcción e Ingeniería de Fabricación, Universidad de Oviedo, Spain

ABSTRACT

Ball mills have a low efficiency rate partially due to the lack of a proper method to monitor the mill filling level, which makes it difficult to control the grinding process. The purpose of this paper is to explore the possibilities that DEM offers to characterize the load torque of tumbling ball mills in the frequency domain and, from this characterization, to establish the basis of a methodology capable of estimating the mill filling level. To achieve this, a pilot scale ball mill was considered and a campaign of simulations and experimental tests was carried out in dry grinding conditions, considering variables such as the rotation speed of the mill, the type of particle to be grinded, and the mill filling level. For each simulation, spectral analysis of torque data generated by DEM software was performed.

The results obtained from simulations and subsequent torque data processing show the possibility of characterizing the load torque of ball mills in the frequency domain without the influence of components alien to the grinding process. In this paper, it is shown that load torque signal in ball mills contains enough information to characterize, unambiguously, the load level of the mill. Thus, a methodology to evaluate the mill filling level based on torque spectral analysis is proposed.

© 2017 The Author(s). Published by Elsevier B.V. This is an open access article under the CC BY-NC-ND license (http://creativecommons.org/licenses/by-nc-nd/4.0/).

1. Introduction

The mining industry would save about 70% of the energy involved in grinding processes if this energy was reduced to its practical minimum energy consumption [1]. In this context, achieving a more efficient grinding in ball mills is an important issue, since these devices have a low efficiency rate partially due to the difficulty to monitor the mill filling.

For a given amount of balls, if the fill level of ore is low, most of the energy of the balls is lost in impacts between them, leading to low comminution ratios. On the other hand, if the mill is overloaded, the grinding material causes a damping effect that decreases the comminution ratio. In between these situations, optimum values of the fill level allow operating the mill at maximum comminution ratios. For this reason, a proper monitoring of the fill level would allow operating the mill at maximum efficiency rates [2].

The difficulty to accurately determine the fill level of ball mills is revealed by the complexity of the control of the grinding process, [3–7]. There are two factors that contribute largely to this. One of them is the

difficulty to place sensors inside the mill to provide halfway information between the input and output of the material [3]. The other factor is the complexity of the dynamical characteristics of the grinding process (the movement of the material within the drum, the size distribution of the ore particles, jams of material, the rotating speed of the mill, etc.) which makes it extremely difficult to obtain an accurate mathematical model of the process [4–6], [8–10]. As a consequence, existing techniques to estimate the filling level have been obtained experimentally and need to combine several duty parameters of the mill, such as pressure difference, outlet temperature, inlet negative pressure or drive current among others. These variables can be affected by several operating conditions apart from the load level; so, to estimate the mill filling level it is needed that the values of these parameters be divided into several grades and then, the working conditions of the mill be empirically evaluated by the combination of these grades [11].

Alternative methods to estimate the filling level based on vibration measurement have been studied. Through successive analysis of the vibration, this variable has been correlated with the filling level on different operating conditions [11–16]. This method shows a high sensitivity to the location of the accelerometers on the structure of the mill [13], which can condition the estimation of the filling level. Some attempts have been made trying to circumvent this problem by combining vibration and

acoustic measurements [12,14,17]; however, the procedure becomes more complex and the noisy operating conditions of this type of machinery can make it difficult to draw firm conclusions [11]. Other methods proposed for mill filling estimation have included techniques based on X-rays [18], force [19] or inductivity [20,21]. In [22], a torque based method is presented, but the results do not show conclusive correlation between the mill filling level and torque harmonics.

Over the last few decades, the discrete element method (DEM) has played a very significant role in the study and characterization of comminution processes, as it is summarized in [23]. This time, it has been proven the ability of DEM to predict the behaviour of grinding devices, such as ball mills. In some cases, this simulation method has been used to extract information that would not be feasible to obtain experimentally. This is the case of particle dynamics [24], particle mixing [25–29] or energy estimation of the comminution process [30]. DEM has also been used to predict the behaviour of torque and power draw [31]. Thus, it has been possible to explore how these variables are affected by: mill operating conditions and liner geometry [32], charge composition and its size distribution [32,33] or lifter height [34]. There can also be found applications of DEM in which the behaviour of the mill at startup is studied [35] and comparative studies of power draw between different mills [36].

The study presented in this paper tries to provide an appropriate response to a real question, which is how to determine the load level of a ball mill. For this purpose, the following hypothesis is formulated: if the mill filling increases this effect will be noticed as a modification in the spectrum of the torque signal of the mill. Two facts support this hypothesis. The first one is the dampening effect created on the grinding media by the particles to be grinded [2,45]. The second one is that, according to the valuable studies performed in [11–13], [15] the higher the mill filling level, the lower the vibration level. The collisions between particles (both balls and grinding material) and the mill shell generate forces which are directly related, not only with vibration, but also with the mill load torque. As a consequence, it is reasonable to assume that the dampening effect accompanying the variation on the mill filling level give rise to a modification in the spectrum of the torque signal.

So far, neither the torque obtained from the simulation of ball mills in the frequency domain nor its correlation with the filling level has been studied. Thus, in this paper, the feasibility of detecting the mill filling level through torque measurement is explored. The measurement of such a variable in industrial environments is not always possible, since very sensitive and expensive sensors are required. Nevertheless, this magnitude is directly related with other electric magnitudes of the motor driving the mill [37], so if the possibility of correlating torque and filling level could be demonstrated that would open the door to the estimation of the filling level through the electric magnitudes of the motor (i.e. voltages and currents). For this reason, the results presented in this paper, correlating torque and mill filling, should be considered in the context of a wider research, the ultimate purpose of which is the optimization of ball mills efficiency through the estimation of the filling level by means of monitoring the electric variables of the drive.

2. Torque in tumbling ball mills

For a specific load and operating conditions, the torque appearing in a tumbling ball mill is a highly variable magnitude in the time domain. This fact is due to the operating principle of ball mills, which is based in the elevation process of balls and material from the toe region to the shoulder region of the drum. Following the elevation process, the consequent fall of the particles inside the mill generates impacts among them and collisions against the drum, which are both inherent to the comminution process. According to this operating principle, the instantaneous value of torque, $T(t)$, can be expressed as the sum of two terms: T_c and $T_f(t)$. The term T_c is a constant value which represents the average torque and is mainly related to the elevation process of the
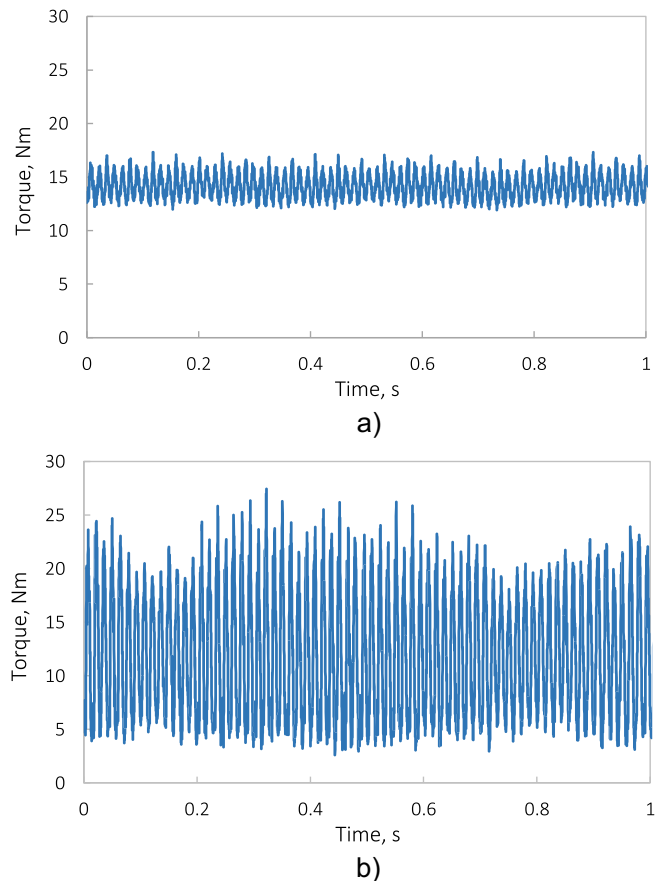

Fig. 1. Time domain records of torque in the shaft of an electric motor rated 2.2 kW driving a constant torque load (a) and a ball mill (b).

load and to the power drawn from the drive. The term $T_f(t)$ is a fluctuating component with a zero mean value. It represents the oscillatory component of the torque and is directly related to repetitive movements of load and to impacts and collisions happening inside the mill provoking sharp variations of the torque and, in turn, of the power draw [31]. This is one of the reasons why ammeter readings of supply current, in motors driving ball mills, show large oscillations. In practice, T_c can be measured or estimated by means of proper instrumentation (load cells and torque transducers) [35]. $T_f(t)$ is more difficult to characterize, since, leaving aside the large and sudden variations of this term due to the grinding process, it always contains other oscillatory components. These components are mainly due to two reasons. One of them is that electric motors add harmonics to torque signal as a consequence of
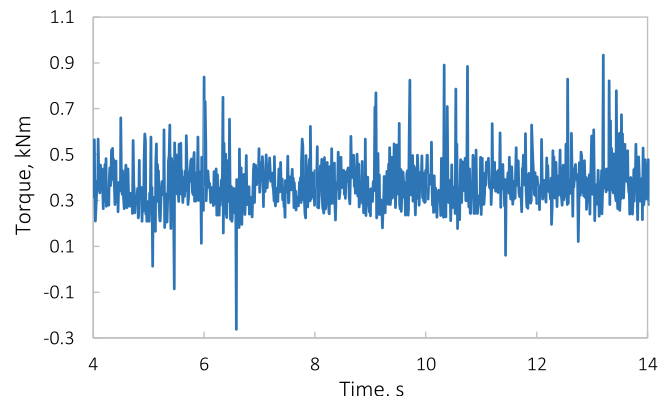

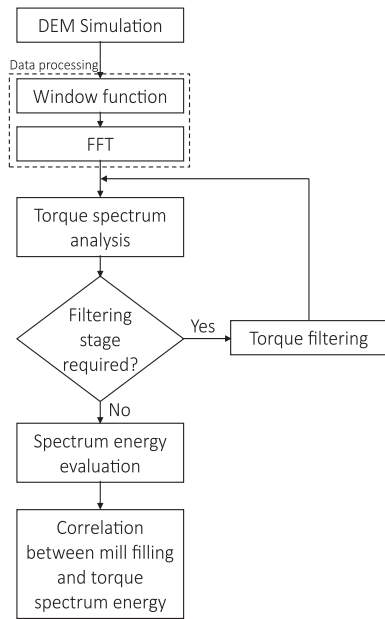**Fig. 2.** Torque data obtained from DEM simulation.

Fig. 3. Flowchart for the study of DEM torque data.

Table 1
Mill dimensions.

Internal diameter, mm	880
Internal length, mm	315
Number of lifters	16
Lifter dimensions (l/w/h), mm	315/30/20
Ball density, kg/m^3	7860
Average ball filling degree, % volume	19.3
Rotation speeds, % critical	62/71/80

DEM simulation (Fig. 2). These data are converted into the frequency domain by applying the Fast Fourier Transform (FFT) and the spectra are subsequently analyzed. The eventual application of a filtering stage and the calculation of torque energy spectra will lead to conclusions about the behaviour of torque as a function of the mill filling level (Fig. 3).

3.1. DEM modelling

DEM is a suitable tool for the study and characterization of ball mill behaviour, since it is a numerical technique especially intended to simulate interacting particles [39]. The DEM algorithm models the collisional interactions of particles using a contact force law, and resolves the particles motion using Newton's laws of motion. For the purpose of this study, the collisional forces have been modelled by employing a Hertz-Mindlin no slip model [40]. In this model, the normal and tangential forces resulting from the particle collisions are calculated by means of the Hertz's elastic contact theory and Mindlin's improvement, respectively. Both forces have damping components which are a measure of the damping property of materials and are related to the coefficients of restitution [41].

According to this model [40] the elastic force component in the normal direction is given by

$$F_{ne} = \frac{4}{3} E^* \sqrt{R^*} \delta_n^{\frac{3}{2}} \tag{1}$$

F_{ne} being the normal force, E^* the equivalent Young's modulus [40], R^* the equivalent radius [40] and δ_n the normal overlap between colliding particles.

The damping force component in the normal direction, F_{nd}, is given by

$$F_{nd} = -2\sqrt{\frac{5}{6}} \beta \sqrt{S_n m^*} \overline{v_n^{rel}} \tag{2}$$

where $\overline{v_n^{rel}}$ is the normal component of the relative velocity, m^* is the equivalent mass, β depends on the coefficient of restitution ε according to

$$\beta = \frac{\ln \varepsilon}{\sqrt{\ln^2 \varepsilon + \pi^2}} \tag{3}$$

and the term S_n is the normal stiffness, given by.

$$S_n = 2E^* \sqrt{R^* \delta_n} \tag{4}$$

both their constructive characteristics and their principle of operation [38]. Beside this, the other cause of oscillatory components is the presence of mechanical devices in the torque transmission chain, such as gears, pinions and crowns, which are used to increase the torque delivered by the electric drive [38]. Both components can be observed in Fig. 1. This figure shows two time domain records of torque measured in the shaft of an electric motor rated 2.2 kW. By means of a flange type torque sensor, the torque signal is recorded when the motor is driving a constant torque load, (Fig. 1(a)), and a ball mill, (Fig. 1(b)). The presence of an oscillating component of around ±2 Nm, superimposed to the average value, can be observed in the case of constant torque load. In the case of the ball mill, much larger oscillations arise. These oscillations are quite irregular in time and especially affect the maximum value, which can reach 27 Nm, i.e. more than 100% of the average value.

The issues exposed above contribute to smearing $T_f(t)$, which, in practice, appears as a combination of related and non-related grinding components. This fact makes extremely difficult to correlate this component with mill charge dynamics, comminution process or mill operating conditions. Specifically, the characterization of $T_f(t)$, which is strictly created by the load of balls and material in a tumbling ball mill, is only possible to be made by means of simulation tools.

3. DEM modelling and data processing

The methodology proposed in this study to characterize the load torque of a ball mill is based on the use of torque data obtained from
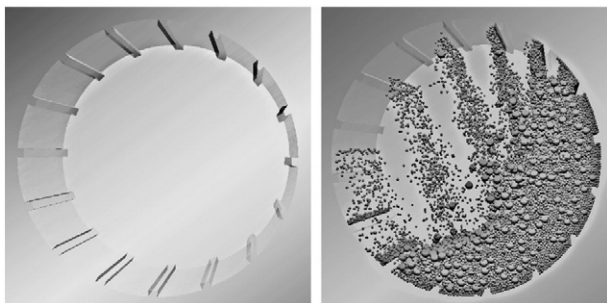

Fig. 4. Mill geometry (left) and loaded mill (right).

Table 2
Material parameters.

	Ceramic	Steel
Density (kg/m^3)	2800	7860
Shear modulus (GPa)	1.6	81
Poisson's ratio	0.22	0.3

Table 3
Coefficients of restitution and friction.

	Ceramic		Steel	
	Restitution	Friction	Restitution	Friction
Ceramic	0.3	0.66	0.2	0.4
Steel	0.2	0.4	0.5	0.15

The elastic component of the tangential force, F_{te}, is given by

$$F_{te} = -S_t \delta_t \tag{5}$$

δ_t being the tangential overlap and S_t the tangential stiffness, which is given by

$$S_t = 8G^* \sqrt{R^* \delta_n} \tag{6}$$

G^* being the equivalent shear modulus.

The tangential component of the damping force, F_{td}, is given by

$$F_{td} = -2\sqrt{\frac{5}{6}}\beta\sqrt{S_t m^*}\overline{v_t^{rel}} \tag{7}$$

where $\overline{v_t^{rel}}$ is the tangential component of the relative velocity. The total tangential force, F_t, is limited by the Coulomb frictional criterion:

$$F_t \leq \mu_s F_n \tag{8}$$

where μ_s is the coefficient of static friction and F_n the total normal force.

3.2. Data selection and processing

For each simulation timestep, DEM allows to obtain the instantaneous torque exerted on the mill, which is the result of adding the individual torques caused by each particle forces and collisions. From these values of instantaneous torque (time domain), a block of data over a certain time window is chosen to perform the conversion into the frequency domain. In order to make valid comparisons between cases with different rotational speeds and different particle distributions, the block of data should be selected in such a way that it is not affected by any substantive segregation [32]. Beside this, there are two issues to take into account when selecting the block of data. One of them is the necessary time for the mill to reach the equilibrium at the start of the simulation. This is the reason why the results obtained during the first seconds of each simulation should be omitted [32]. The second issue is the desired spectrum resolution, which affects the length of the block of data according to

$$\Delta f = \frac{1}{TR} \tag{9}$$

Δf being the spectrum resolution and TR the length of the block of data (also known as time record).

For the purpose of this study, a resolution of 0.1 Hz is considered enough, so a ten-second time record is required. Therefore, to take into account all the above restrictions to select the block of data, the time period is chosen to be between 4 and 14 s for almost all cases. The data samples are equally spaced 10 ms, which, according to Nyquist criterion, allow to characterize the signal in the frequency domain up to

Table 4
Cases analyzed.

	Rotation speed (%W_C)		
Particle density	80	71	62
High	HDHS#X	HDMS#X	HDLS#X
Low	LDHS#X	LDMS#X	LDLS#X

Table 5
Load levels.

Load level identification	#1	#2	#3	#4	#5	#6	#7
Number of particles	4062	8124	12,186	16,248	20,310	24,372	28,434
Particle filling, %	40	80	120	160	200	240	280
Fill level, % mill volume	3	6	10	13	16	19	23

50 Hz. Before performing FFT analysis, a window function is applied to the block of data to avoid spectral leakage effect. This means that the FFT is applied on the result of multiplying every sample of the block of data by the corresponding value of the window function. In this work, a Hann window function, $W(n)$ is used

$$W(n) = \sin^2\left(\frac{\pi \cdot n}{N-1}\right) \tag{10}$$

where N is the number of samples of the time record and n is comprised between 0 and N-1.

4. DEM model and simulations

The DEM model of the ball mill used in this study has been developed using EDEM® software package. The ball mill used in simulations is based on a laboratory unit composed of a cylindrical drum with a set of 16 uniformly distributed lifters (Fig. 4). To establish the dimensions and ball load of this mill, the characteristics of other mills used in previous studies [13,21,43], have been taken into account. In these cases, despite the fact that the mills do not have large dimensions, they have been proven to deliver reliable and useful results in laboratory tests. The main dimensional data of the mill used in this work are summarized in Table 1. To act as a grinding media, the ball load is composed of a set
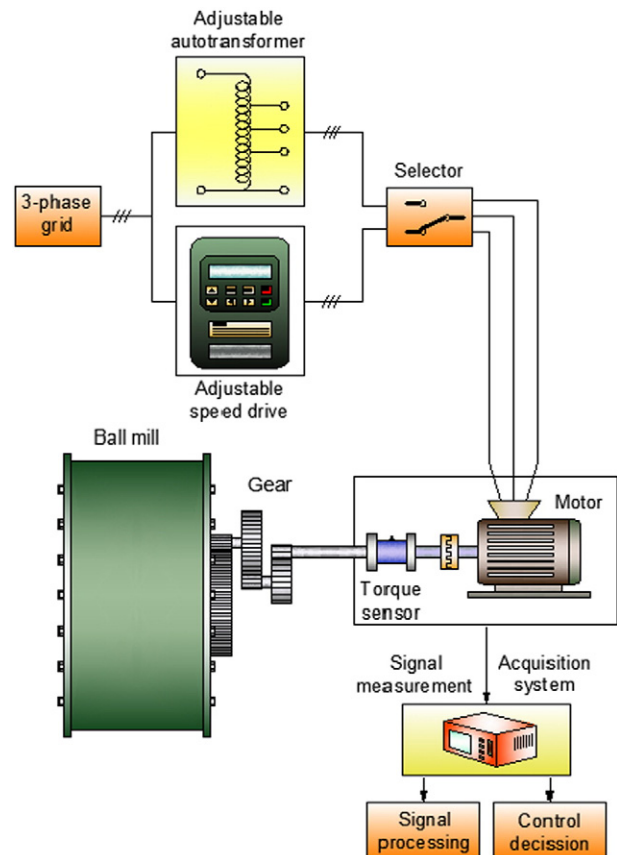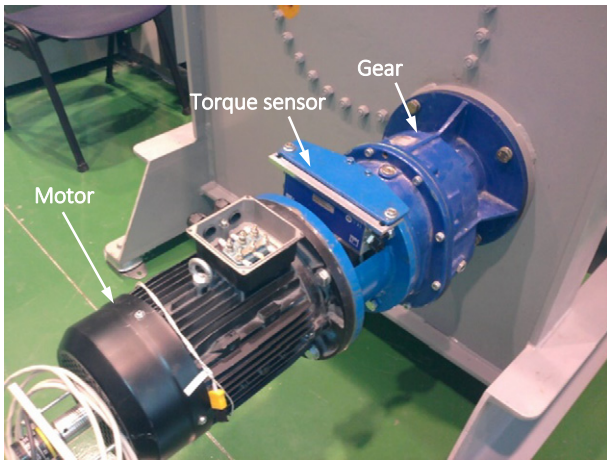

Fig. 5. Test rig scheme.

Fig. 6. Rear view of the ball mill showing the electric motor, the torque sensor and the gear.

5. Experimental tests

To validate the proposed methodology, a test rig based on a monitored ball mill has been used. This ball mill ~~mil~~ has the same characteristics and dimensions of the DEM model specified in Table 1. In Fig. 5, it is shown a diagram including the main components of the rig. The mill is driven by a three-phase, four-pole, 400 V, 50 Hz, 2.2 kW, induction motor. As it is shown in Fig. 6, the motor shaft is coupled to a HBM™ flange type torque sensor which provides accurate torque measurements. This device is coupled to the mill through a three stage reduction gear set with a total gear ratio of 36.27. Thus, the motor torque can be increased up to the value needed to drive the mill. Gears are universally used in mills and they have an important effect on torque harmonics [44]. For this reason, it is important for the test rig to include such significant devices in the same way as they are used in industrial facilities. To drive the mill at the selected speeds, the electric motor is fed by means of an adjustable speed drive (ASD). Moreover, the test rig also includes an autotransformer to feed the motor with voltages under its rated value. This particular low voltage operation strategy is part of the test procedure and takes place at the beginning of each test, as discussed below. The data acquisition system monitors the following variables of the motor: voltages, currents, torque, speed, vibration and temperature. Fig. 7 shows an overview of the test rig.

Two important aspects concerning the test rig and the procedure followed in the experimental tests need to be commented. One of them is that the ball mill used in both simulations and lab tests has a similar diameter to the one used by small industrial mills. This fact makes the results comparable to those that can be obtained in industrial facilities. The second aspect is that, in order to make the most reliable comparisons among torque spectra for different filling levels, the influence of motor temperature on torque has been taken into account. As depicted in Fig. 8, after the start-up of the motor, a thermal transient period takes place until reaching a stabilized temperature. During this transient period, the fluctuations of torque due to temperature drift can be significant. Thus, in order to obtain comparable data, measurements should be made only once the temperature has reached steady state. However, if the mill were running until reaching this temperature, torque measurements could be affected by segregation of particles, which would make the comparisons less reliable. To avoid the undesirable influence of both segregation and thermal transient, the motor was warmed up before starting each test. With this aim, the motor was fed at reduced voltage by using an autotransformer until reaching the desired temperature but without producing enough torque to start the mill.

of 2466 steel balls which represent a 19.3% of the internal volume of the mill. The simulations performed in this work combine two different types of material to be grinded with three different rotation speeds. The study of two materials with very different characteristics and densities, such as ceramic-like (2800 kg/m^3) and steel-like (7860 kg/m^3) particles, was considered of interest. The material parameters used in simulations are specified in Table 2. In Table 3, the coefficients of restitution and friction between each pair of materials are detailed. It is considered that the mill is made of steel. The rotation speeds were selected according to the criterion used in mineral processing plant design by taking into account the internal diameter of the mill. As it is specified in [42], for ball mills with internal diameter lower than 1.8 m, a maximum of 80% critical speed was chosen. Thus, this was the maximum speed used in simulations. Beside this, 71% and 62% of the critical speed were also simulated.

Table 4 shows the matrix of cases simulated with the nomenclature which is referred to throughout this paper. Beside the four-letter code identifying each case, the term #X represents a number in the range of 1 to 7, which identifies the load level of the mill as it is shown in Table 5. These load levels refer to the particle filling used during simulations. Particle filling is defined as the fraction of void spaces within the resting ball load that are filled with the particles to be grinded [21].

Fig. 7. Test rig overview. Left: Ball mill inside its soundproof room. Right: Control and measurement post next to the soundproof room.
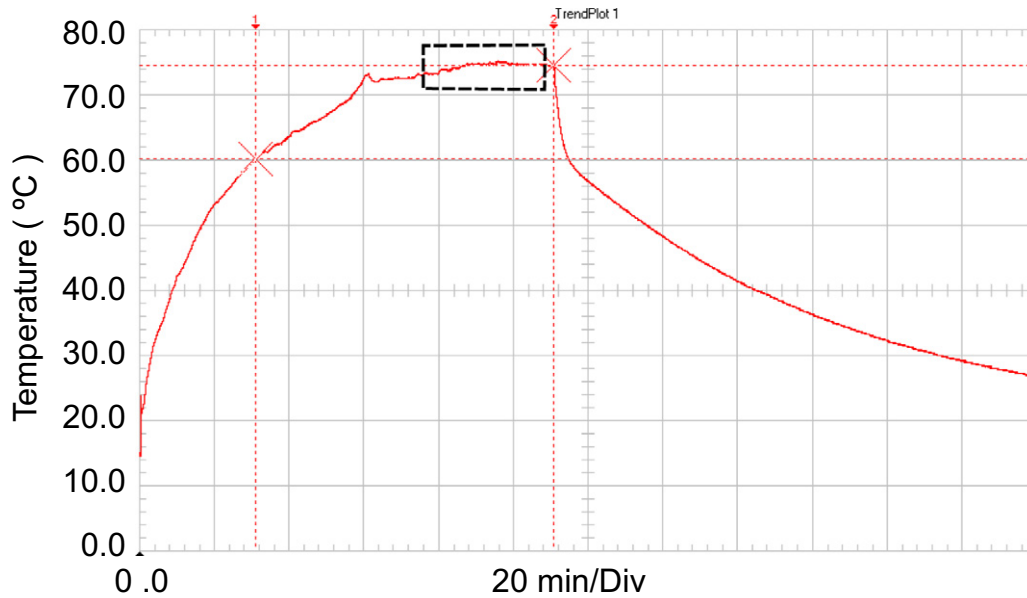
Fig. 8. Evolution of motor temperature in a complete warming and cooling cycle. The box shows the zone in which measurements should be taken.

6. Results and discussion

The cases exposed in Table 4 have been simulated and every set of torque data has been analyzed according to the methodology proposed in Fig. 3. The average torque has been calculated and spectral analysis in the low frequency range (up to 50 Hz, which is the limit imposed by the sample frequency used in DEM simulations) has been performed in all cases. The main results are discussed below.

6.1. Average torque

The power consumption of the electric motor driving a ball mill has low sensitivity to detect variations in the quantity of material to be grinded (i.e. mill filling) [14]. This lack of sensitivity is due to the fact that the load of balls in these mills is so large that it is responsible for most of the power demand. Thus, large variations cannot be found in this variable from underfilling to overfilling conditions. Beside this behaviour, other reason contributing to the low sensitivity of power is the saturation effect appearing in the power consumption when the mill is overfilled [2,21]: for large filling levels a decreasing tendency on power appears. Since a straightforward relationship exists between the power consumption and the required torque, the same behaviour as explained above for power can be expected for torque at constant speed.

In Fig. 9, the average torque vs. mill filling level is plotted for all the case studies. The values of torque are expressed in per unit of the maximum value of torque for every case. As expected, in all of them torque increases from the lowest fill level, then a maximum value is reached which is followed by a decreasing tendency of the torque for the highest fill level. The maximum variation of torque observed for all the fill levels is below 9% of the maximum torque. Thus, the results obtained from the DEM model corroborate the expected lack of sensitivity of torque in evaluating the fill level. The tendency to saturation of torque is also the expected result.

6.2. Lifter torque harmonic

The effect of a lifter coming in and out in the bulk of balls and particles to be grinded can be assimilated to an alternating increase and

decrease of torque. So, from the point of view of torque, a lifter torque harmonic (LTH) is expected to appear at frequency $n \cdot w$, n being the number of lifters inside the mill and w the rotation speed expressed in Hz. This LTH can be clearly identified in the torque spectra as it can be seen in Fig. 10. The spectra shown in this figure correspond to the simulations of HDMS filling levels and in these cases, LTH appears at 8.8 Hz, which is the frequency corresponding to a rotation speed equal to 71% of the critical speed. At the lowest load level, the spectrum is very noisy and LTH is not much evident, but as the load level increases LTH becomes more and more remarkable. This fact is in part due to the decreasing noise level for increasing loads, as it will be analysed in the next section.

LTH appears in all the cases analyzed independently of rotation speed, type of load or filling level. The analysis of all the spectra reveals that the amplitude of this harmonic is variable but it does not show a monotonic tendency or correlation with increasing filling levels. LTH amplitude as a function of the filling level is shown in Fig. 11, where the behaviour of this harmonic in all the case studies is summarized. As it can be seen, LTH undergoes increasings and decreasings apparently not related to the mill filling. A possible explanation to this behaviour can be based on the combination of the unsteady flow of charge in the
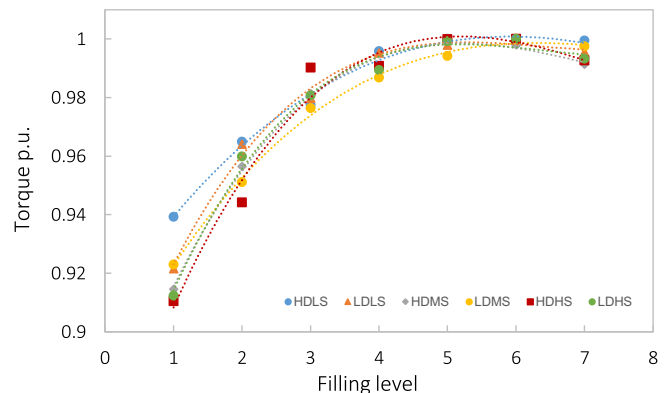

Fig. 9. Average torque (in per unit of the maximum value) vs. mill filling level for all the case studies.
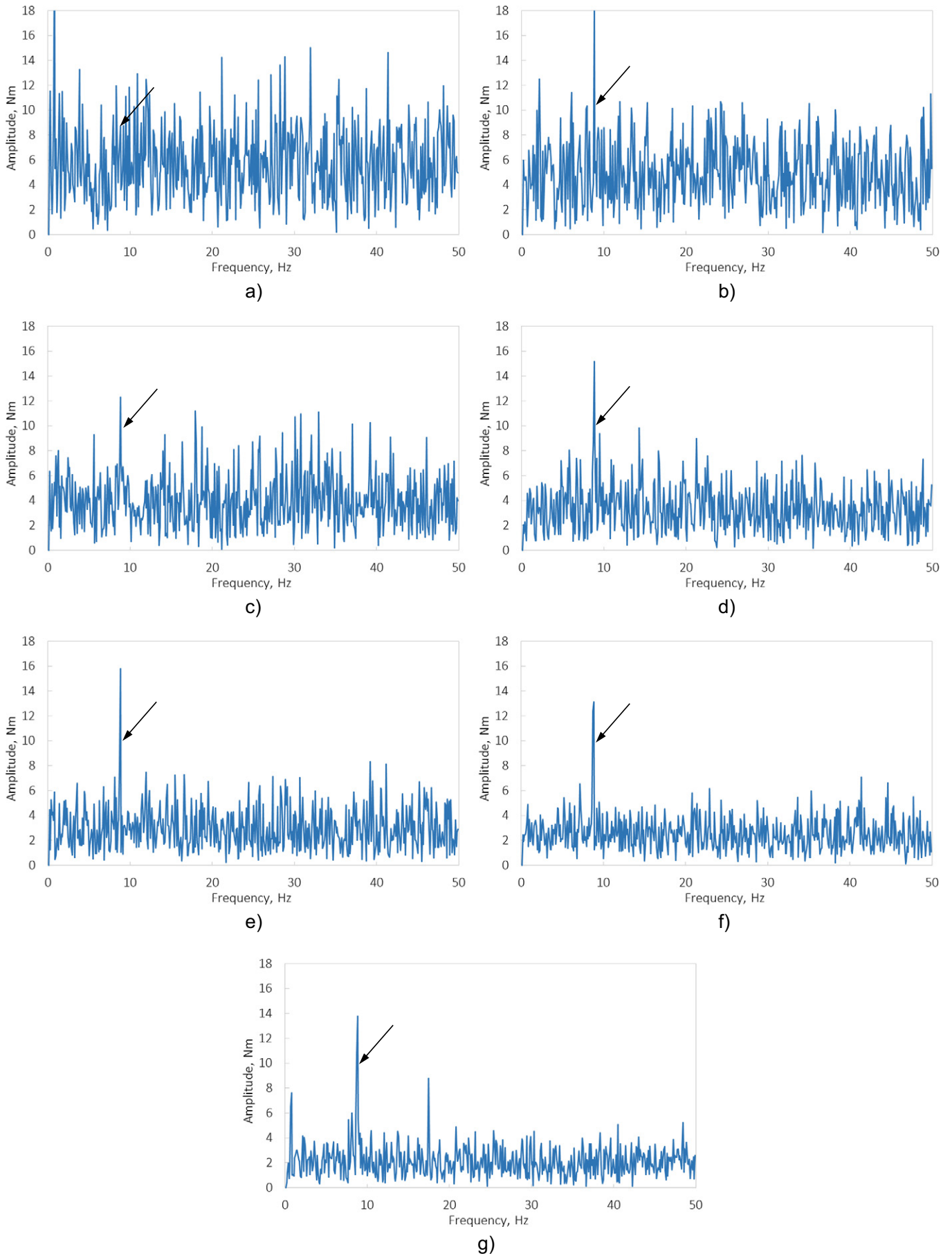
Fig. 10. HDMS torque spectra with arrows marking LTH: a) HDMS1, b) HDMS2, c) HDMS3, d) HDMS4, e) HDMS5, f) HDMS6, g) HDMS7.
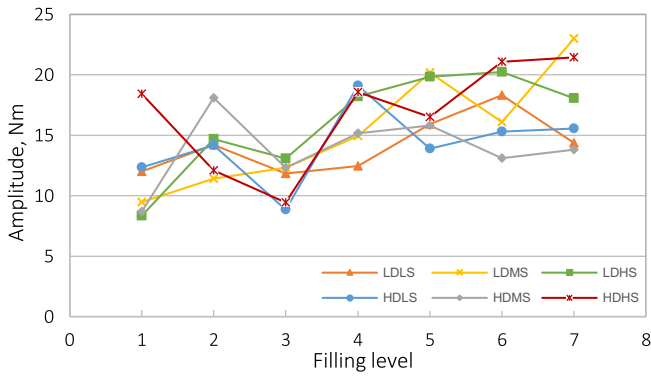
Fig. 11. Lifter torque harmonic evolution.

mill, the nature of LTH, and the length of the time record. In the block of data shown in Fig. 2, it can be observed that torque undergoes strong variations which reveal the impulsive and unsteady features of the charge flow. Beside this, LTH is only due to a small part of the bulk present in the mill, which is largely affected by that unsteady characteristic of the charge flow. Both reasons justify that LTH presents fluctuations non-dependent on the mill filling. It is possible that, if much larger time records were used, this behaviour would not appear, since, statiscally, the strong variations would be smoothed. Nevertheless, this possibility is not very useful in practical terms, because, if much larger time records were necessary, the practical application of the method would become unfeasible.

6.3. Spectrum noise

A major advantage of DEM simulation is that it makes possible to perform a study of the torque due exclusively to the grinding phenomena, i.e. the torque obtained from DEM is free of any influence from gears and driving motor harmonics. For this reason, the level of noise detected in torque spectra is mainly due to the grinding conditions.

In Fig. 10, it can be observed that the overall amplitude of torque spectra show a clear tendency to decrease as the mill filling increases. To provide a more meaningful view of this behaviour, a 3-D representation of spectra is shown in Figs. 12 and 13. These figures give a graphical portrayal of the spectra obtained in the cases presented in Table 4. For each case, the spectrum obtained for every filling level is shown in an increasing order, providing a waterfall-type representation of the spectra evolution. These figures make explicit the erratic behaviour of LTH amplitude, which is always the more significant harmonic closest to 10 Hz. Besides this, a confirmation of the decreasing tendency of the overall amplitude of torque spectra as the mill filling increases can be observed. It can also be seen that the noise level of the torque spectra follows the same pattern in all cases for each rotation speed and type of load: the noise level decreases as the mill filling increases even for filling levels much higher than those used in actual working conditions.
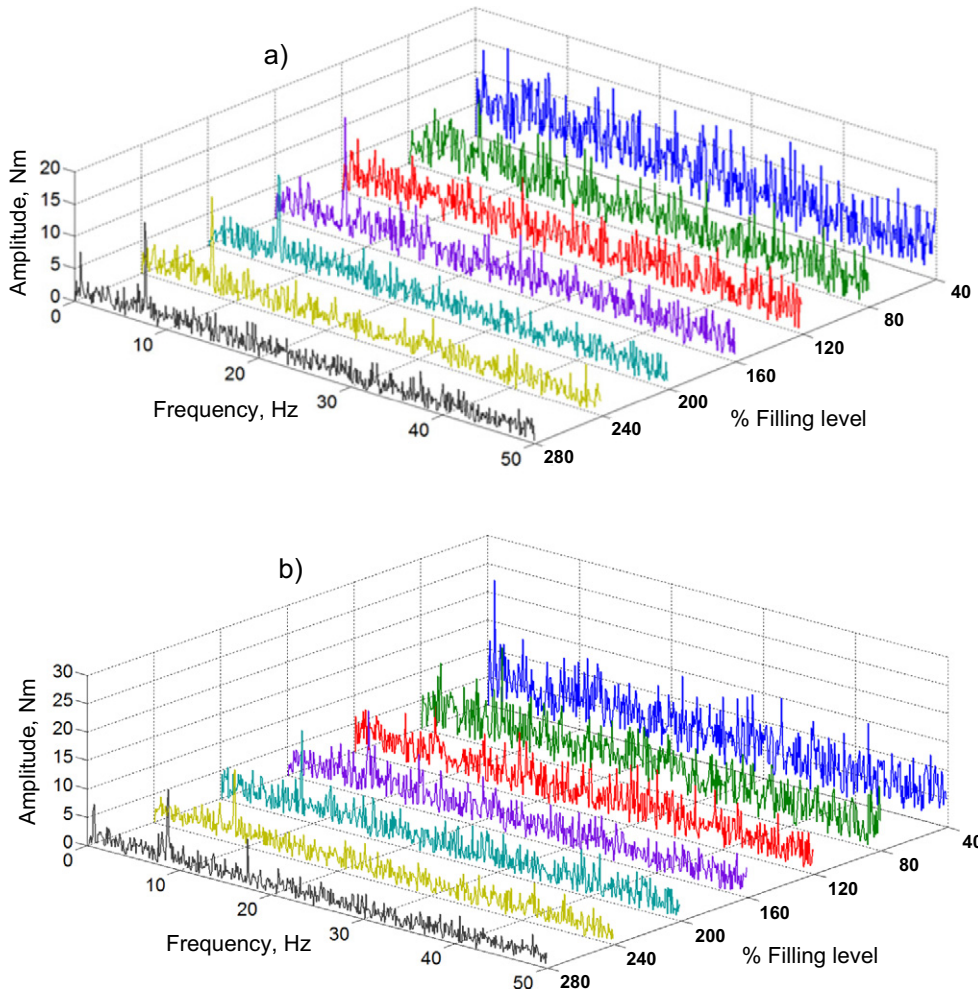

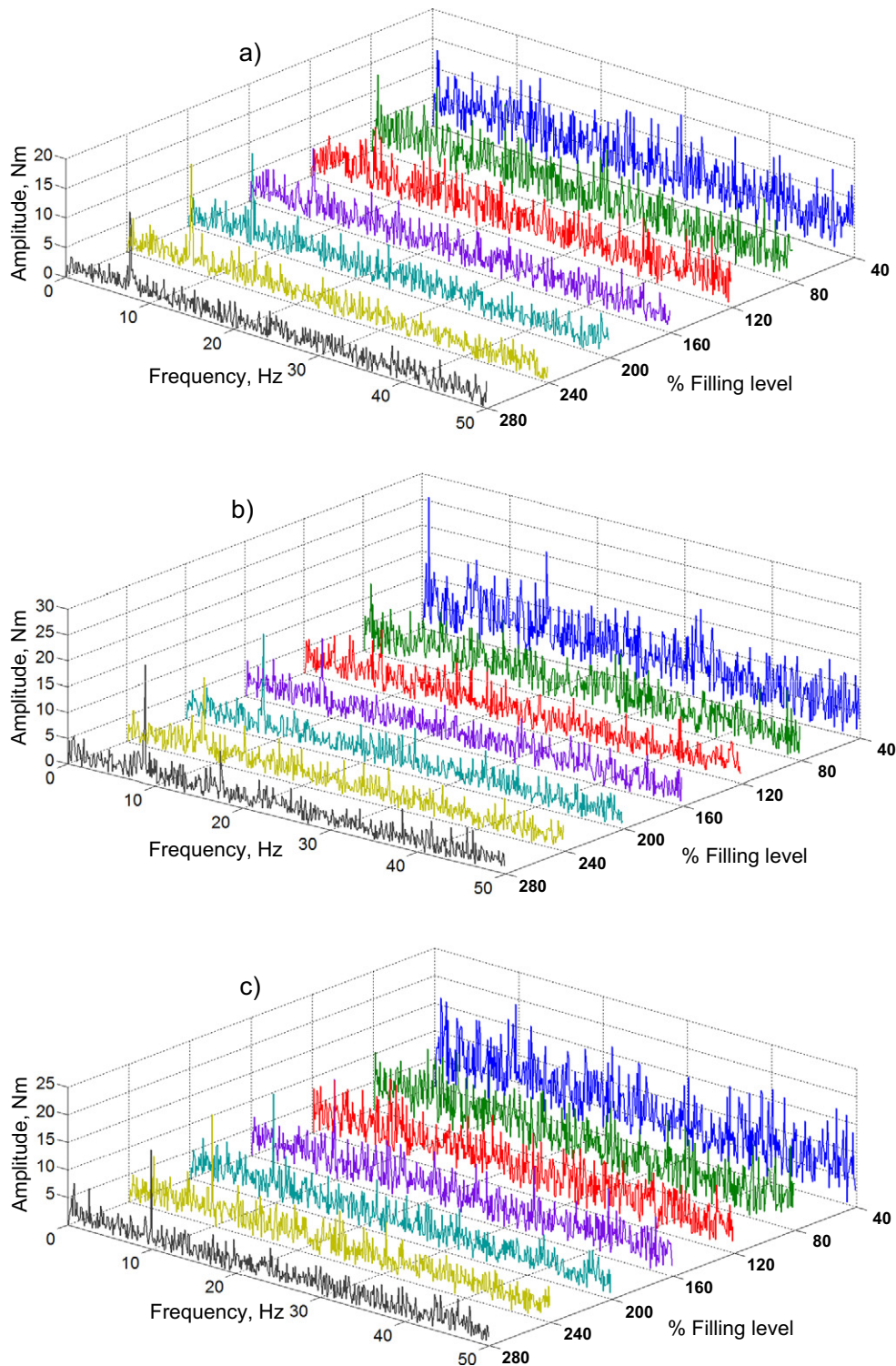**Fig. 12.** Waterfall representation of torque spectra: a) HDLS, b) HDHS.

Fig. 13. Waterfall representation of torque spectra: a) LDLS, b) LDMS, c) LDHS.

This tendency of the noise level is justified by the buffer effect of an increasing load on the interaction of particles. At low material filling level, ball-to-ball impacts predominate. Since these interactions have high restitution coefficients, then high force pulses will be translated into high torque pulses on the mill geometry. As a consequence, this fact will increase the noise level of torque signal.

In the case of mill overfilling, the situation is just the opposite since a buffering effect appears affecting balls and material collisions. The ball-to-material impacts and material-to-material impacts predominate in this case and both interactions present restitution coefficients much lower than ball-to-ball impacts. Then, lower force and torque pulses are exerted on the mill geometry and the noise level of torque decreases.
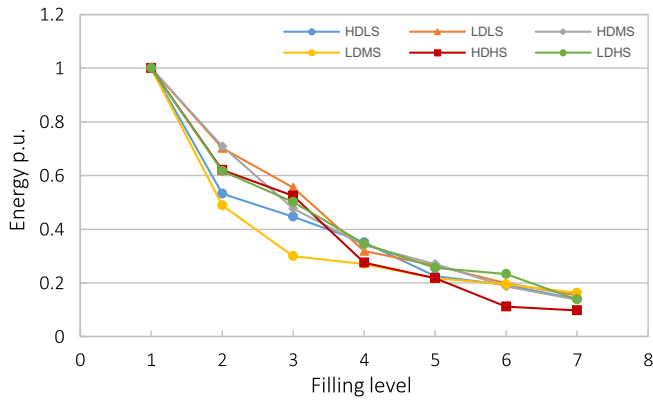
Fig. 14. Spectrum energy (in per unit of the maximum value) vs. filling level.

Table 6
Curve fitting equations.

Case	Equation	R^2
HDLS	$y = -0.423\ln(x) + 0.9279$	0.9650
LDLS	$y = -0.451\ln(x) + 1.0057$	0.9881
HDMS	$y = -0.454\ln(x) + 0.9987$	0.9959
LDMS	$y = -0.408\ln(x) + 0.8738$	0.8982
HDHS	$y = -0.476\ln(x) + 0.9868$	0.9849
LDHS	$y = -0.429\ln(x) + 0.9646$	0.9882

Between the above situations, all the intermediate cases can be justified in the same way: the different rates of balls and material give rise to combinations of more or less buffered impacts and to the subsequent less or more noisy torque spectra.

6.4. Mill filling monitoring by means of torque

From the waterfall representation in Figs. 12 and 13, it can be deduced that a high correlation exists between the torque signal due to the grinding process and the fill level of the mill. Specifically, the pattern shows a continuous decreasing of noise as the load increases; so, at this point, a quantification of this feature will be done according to the flowchart proposed in Fig. 3.

A previous consideration to the evaluation of the noise is to perform a filtering of torque signal. As it has been explained, neither the mean value of the signal, nor LTH harmonic, contribute to characterize properly the mill filling level. Then, the purpose of the filtering task is the elimination of both signal components.

Once the torque signal has been filtered, the quantification of the noise level can be done in terms of the energy of the signal according to the following expression:

$$E_t = \int_{t_1}^{t_2} |X(t)|^2 dt \qquad (11)$$

where E_t is the total energy of the signal between the instants t_1 and t_2 and $|X(t)|$ is the modulus of the signal to be evaluated. The calculation of E_t has been done for every case study in Table 4 and the results can be observed in Fig. 14. In order to facilitate comparison, the energy expressed in per unit of the maximum value (i.e. the energy obtained for the minimum load level simulated) as a function of the load level has been represented for every case. This graphical representation
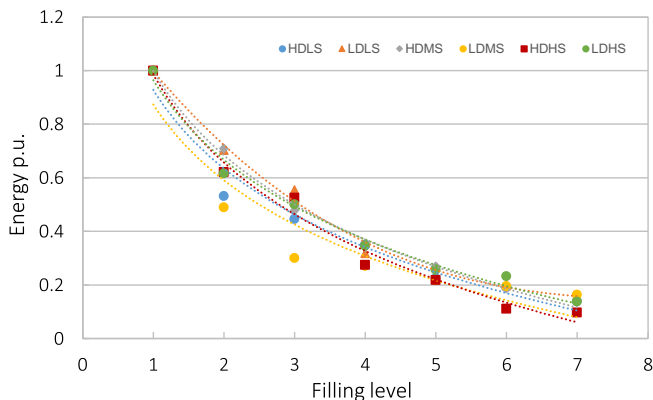
confirms the tendency observed in the waterfall representation of the spectra; since, as the load level increases, the energy of the signal clearly decreases monotonously. This is a significant result, since through the quantification of the energy of the torque signal, the load level of the mill can unambiguously be identified. So, despite the apparently insensitivity of torque to distinguish the filling level (when attention is paid only to averaged torque) it can be concluded that torque signal contains enough information to identify the load level and this information can be obtained if a proper treatment of signal is done.

In all cases, the simulation results show a more accused drop of the energy of the signal at the lowest load levels, which becomes smoother for higher load levels. A good correlation between this behaviour and logarithmic functions can be found (Fig. 15). In fact, very high correlation coefficients are obtained when a logarithmic curve fitting is applied to the energy vs. filling level (Table 6).

6.5. Experimental results

From the point of view of the practical implementation of the method, not all the simulated cases are of interest, such as those conducted at very low rotational speeds or very high filling levels. Such situations are very useful from a theoretical perspective to extract conclusions and to confirm tendencies of the studied magnitudes; however, they are impossible to find in practice since they are infeasible for the real operation of the mill. For this reason, only the more realistic cases have been considered in the experimental tests: the maximum tested mill filling has been 200%, and the rotational speeds have been approximately 80% and 71% of the critical speed. In these cases, the induction motor was fed from the ASD at frequencies of 46 Hz and 41 Hz, respectively. Since the ASD drives the motor in open loop, the mill speed slightly varies with the load, and thus, with the mill filling level.

As it is shown in Fig. 16, the torque spectrum in the span 0 to 500 Hz shows one prominent harmonic. This harmonic is always present on the mill side at the mesh frequency of the pinion and crown. The mesh frequency of a gear is the oscillation frequency due to torsional vibration induced by the stiffness variation of the gear teeth contact [44], which in this case is due to the pinion and crown wheels. This frequency is obtained from the number of teeth of the pinion or the crown multiplied

Fig. 15. Logarithmic curve fitting of energy vs. filling level.
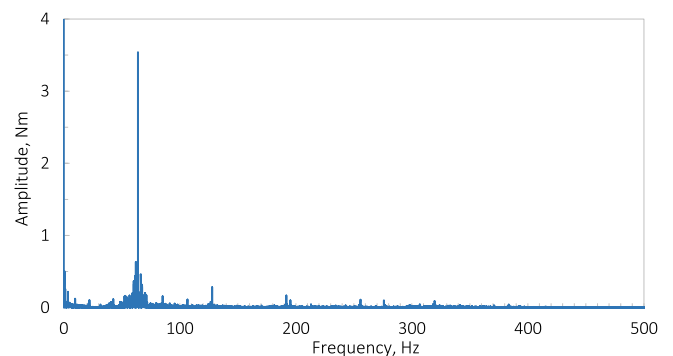

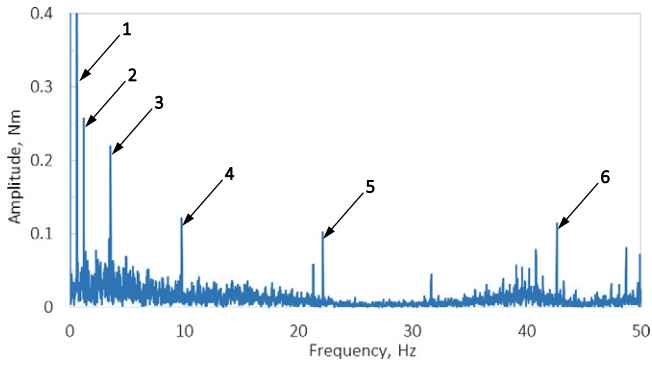Fig. 16. Torque spectrum from lab measurement showing the most prominent harmonic at mesh frequency. Case LDHS#2.

Fig. 17. Torque spectrum showing the main harmonics in the frequency band of interest. Case LDHS#2.

Fig. 18. Spectrum energy of lab test (in per unit of the maximum value) vs. filling level.

by its respective rotating frequency. In the case of the spectrum shown in Fig. 16, the mesh frequency appears at 63.93 Hz, which is the result of 18 teeth of the pinion turning at 3.55 Hz. This harmonic can hide the effect of grinding in the torque signal of actual mills, and thus, it should be filtered in the case it appears in the frequency range of interest (0 to 50 Hz) when applying the proposed methodology. In the case of this study, the mesh frequency is over 50 Hz, so it is out of such a range. Thus, it is not necessary to perform any filtering task on this harmonic.

The relevant harmonics in the range of interest are shown in Fig. 17 and listed in Table 7. As it was predicted by DEM simulation, the LTH is one of them. These harmonics are mainly related to the inherent eccentricity of the rotating elements, and to the electric motor itself. As a consequence, all of them vary their frequencies with the rotating speed, and therefore, with the mill filling level. As in the case of the mesh frequency, these harmonics are either not related with the grinding effect and they smear torque signal. Thus, in order to properly apply the exposed methodology, those harmonics should be filtered before the evaluation of the spectrum energy. Other harmonics not listed in Table 7 are not included in the filtering process because of their small amplitude and, consequently, their minor impact in the evaluation of the spectrum energy of the torque signal.

On the basis of the above considerations, the energy of the torque spectrum, E_t, has been calculated for every experimental test. The results can be observed in Fig. 18, and they confirm the tendency observed in DEM simulations: as the load level increases, the energy of the signal decreases monotonically. These results prove the validity and applicability of the method and demonstrate the ability of the technique to be applied to an actual ball mill in dry grinding conditions. Further comments can be done if the experimental results are compared with those obtained from simulations in terms of specific values rather than on tendencies. In such a case, Fig. 19 shows that the decreasing tendency exhibited by the experimental results is less pronounced than the one obtained from simulations. This is due to the influence of outliers appearing in the simulated torque, which can be observed in Fig. 2. These outliers are also explicit in other works [31,34], and they can have a significant impact in the evaluation of the energy of the fluctuating component of the signal, due to the fact that they present more tendency to appear when the simulation is run with less particles, thus, increasing the energy of such a fluctuating component.

7. Conclusions

There are two factors which make extremely difficult to correlate experimentally torque and filling level in a ball mill. One of them is a saturation effect appearing on torque as the mill filling increases. The other factor is the effect of the gears, always present to multiply the torque of the electric drive, which smear torque signal with non-related grinding components. In this paper, by means of DEM simulation and spectral analysis, it has been shown that it is possible to characterize the load torque of ball mills specifically due to the grinding process in dry conditions. From this characterization, it can be observed that a harmonic related to the rotation speed and the number of lifters, LTH, is always present. If a filtering stage is applied, to eliminate both the average torque component and LTH from the torque data, and a quantification of the energy of the resulting signal is done, a continuous decreasing of the noise level in the torque signal is observed as the mill filling increases.

This fact makes it possible to propose a methodology to evaluate the mill filling level based on torque spectral analysis. Such a methodology has been successfully applied to a pilot mill in lab tests. The results have confirmed the tendency, previously observed in simulations, of the noise level in the torque signal to decrease as the mill filling level increases. Thus, the ability of this indicator to evaluate the mill filling level in dry grinding conditions has been proven.

Table 7
Main harmonics in the 0 to 50 Hz range.

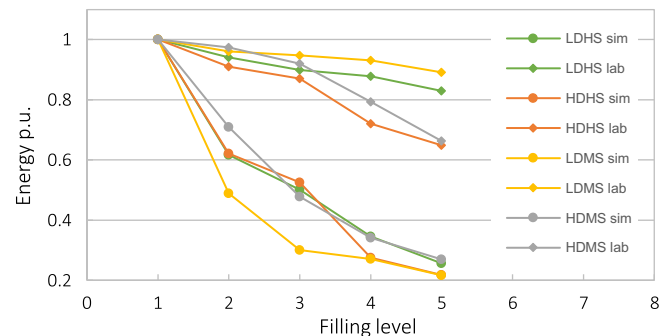|	
Mill turn frequency	#1
×2 Mill turn frequency	#2
Second stage gear output frequency	#3
LTH	#4
Electric motor turn frequency	#5
Mesh-related frequency	#6

Fig. 19. Comparison of spectra energies vs. filling level in simulations (sim) and lab tests (lab).

Discrete Element Method (DEM) simulations and analysis were conducted using EDEM® 2.7 particle simulation academic software provided by DEM Solutions. Ltd., Edinburgh, Scotland, UK.

References

[1] U.S. Energy Department, Industrial technologies program report, Mining Industry Energy Bandwidth Study, 2007.

[2] J. Kolacz, Measurement system of the mill charge in grinding ball mill circuits, Miner. Eng. 12 (1997) 1329–1338.

[3] M. Boulvin, A.V. Wouwer, R. Lepore, C. Renotte, M. Remy, Modeling and control of cement grinding processes, IEEE Trans. Control Syst. Technol. 11 (5) (Sep. 2003) 715–725.

[4] X. Chen, J. Zhai, Q. Li, S. Fei, Fuzzy logic based online efficiency optimization control of a ball mill grinding circuit, Proc. Fourth International Conference on Fuzzy Systems and Knowledge Discovery, FSKD 2007, Haikou, China, Vol. 2, August 24–27, 2007, pp. 575–580.

[5] J. Sue, X. Zhang, X. Zeng, Y. Cui, Design and simulation of robust ball grinding mill control system, Proc. Chinese Control and Decision Conference, 2009. CCDC '09, Guilin, China June 17–19, 2009, pp. 2813–2818.

[6] X. Chen, S. Li, J. Zhai, Q. Li, Expert system based adaptive dynamic matrix control for ball mil grinding circuit, Expert Syst. Appl. 36 (2009) 716–723.

[7] W. Heng, J. Minping, A fuzzy control method for ball mill system based on fill level soft sensor, Proc. Chinese Control and Decision Conference, 2009. CCDC '09, Guilin, China June 17–19, 2009, pp. 5888–5891.

[8] J.L. Salazar, L. Magne, G. Acuña, F. Cubillos, Dynamic modelling and simulation of semi-autogenous mills, Miner. Eng. 22 (2009) 70–77.

[9] H. Benzer, Modeling and simulation of a fully air swept ball mill in a raw material grinding circuit, Powder Technol. 150 (2005) 145–154.

[10] H.J.C. Gommeren, D.A. Heitzmann, J.A.C. Moolenaar, B. Scarlett, Modelling and control of a jet mill plant, Powder Technol. 108 (2000) 147–154.

[11] Z. Su, P. Wang, X. Yu, Z. Lv, Experimental investigation of vibration signal of an industrial tubular ball mill: monitoring and diagnosing, Miner. Eng. 21 (2008) 699–710.

[12] G. Si, H. Cao, Y. Zhang, L. Jia, Experimental investigation of load behaviour of an industrial scale tumbling mill using noise and vibration signature techniques, Miner. Eng. 22 (2009) 1289–1298.

[13] B. Behera, B.K. Mishra, C.V.R. Murty, Experimental analysis of charge dynamics in tumbling mills by vibration signature technique, Miner. Eng. 20 (2007) 84–91.

[14] G. Si, H. Cao, Y. Zang, L. Jia, A new approach to load measurement for industrial scale ball mill, Proc. 2008 IEEE International Conference on Mechatronics and Automation, Takamatsu, Japan August 5–8, 2008, pp. 302–307.

[15] P. Huang, M. Jia, B. Zhong, Investigation on measuring the fill level of an industrial ball mill based on the vibration characteristics of the mill shell, Miner. Eng. 22 (2009) 1200–1208.

[16] S.P. Das, D.P. Das, S.K. Behera, B.K. Mishra, Interpretation of mill vibration signal via wireless sensing, Miner. Eng. 24 (2011) 245–251.

[17] P.R. Aguiar, P.J.A. Serni, E.C. Bianchi, F.R.L. Dotto, In-process grinding monitoring by acoustic emission, Proc. IEEE International Conference on Acoustics, Speech, and Signal Processing, ICASSP '04, Montreal, Quebec, Canada, Vol. 5, May 17–21, 2004, pp. 405–408.

[18] M.S. Powell, G.N. Nurick, A study of charge motion in rotary mills part 2– experimental work, Miner. Eng. 9 (3) (1996) 343–350.

[19] M.H. Moys, J. Skorupa, Measurement of the radial and tangential forces exerted by the load on a liner in a ball mill as a function of load volume and mill speed, Int. J. Miner. Process. 37 (3–4) (1993) 239–256.

[20] K.K. Kiangi, M.H. Moys, Measurement of load behaviour in a dry pilot mill using an inductive proximity probe, Miner. Eng. 19 (13) (2006) 1348–1356.

[21] K.K. Kiangi, M.H. Moys, Particle filling and size effects on the ball load behaviour and power in a dry pilot mill: experimental study, Powder Technol. 187 (2008) 79–87.

[22] P.M. Esteves, M.M. Stopa, B.J.C. Filho, R. Galery, Charge behavior analysis in ball mill by using estimated torque, IEEE Trans. Ind. Appl. 51 (3) (May/June 2015).

[23] N.S. Weerasekara, M.S. Powell, P.W. Cleary, L.M. Tavares, M. Evertsson, R.D. Morrison, J. Quist, R.M. Carvalho, The contribution of DEM to the science of comminution, Powder Technol. 248 (2013) 3–24.

[24] P. Owen, P.W. Cleary, The relationship between charge shape characteristics and fill level and lifter height for a SAG mill, Miner. Eng. 83 (2015) 19–32.

[25] F. Geng, L. Gang, Y. Wang, Y. Li, Z. Yuan, Numerical investigation on particle mixing in a ball mill, Powder Technol. 292 (2016) 64–73.

[26] M. Wu, V. Wang, Modeling ball impact on the wet mill liners and its application in predicting mill magnetic liner performance, Miner. Eng. 61 (2014) 126–132.

[27] G.W. Delaney, R.D. Morrison, M.D. Sinnott, S. Cummins, P.W. Cleary, DEM modelling of non-spherical particle breakage and flow in an industrial scale cone crusher, Miner. Eng. 74 (2015) 112–122.

[28] P.W. Cleary, R.D. Morrison, Understanding fine ore breakage in a laboratory scale ball mill using DEM, Miner. Eng. 24 (2011) 352–366.

[29] S. Rosenkranz, S. Breitung-Faes, A. Kwade, Experimental investigations and modelling of the ball motion in planetary ball mills, Powder Technol. 212 (2011) 224–230.

[30] N.S. Weerasekara, L.X. Liu, M.S. Powell, Estimating energy in grinding using DEM modelling, Miner. Eng. 85 (2016) 23–33.

[31] P.W. Cleary, Predicting charge motion, power draw, segregation and wear in ball mills using discrete element methods, Miner. Eng. 11 (11) (1998) 1061–1080.

[32] P.W. Cleary, Charge behaviour and power consumption in ball mills: sensitivity to mill operating conditions, liner geometry and charge composition, Int. J. Miner. Process. 63 (2001) 79–114.

[33] N. Djordjevic, Influence of charge size distribution on net-power draw of tumbling mill based on DEM modelling, Miner. Eng. 18 (2005) 375–378.

[34] N. Djordjevic, Discrete element modelling of the influence of lifters on power draw of tumbling mills, Miner. Eng. 16 (2003) 331–336.

[35] G.M. Monama, M.H. Moys, DEM modelling of the dynamics of mill startup, Miner. Eng. 15 (2002) 487–492.

[36] R.D. Morrison, P.W. Cleary, M.D. Sinnott, Using DEM to compare the energy efficiency of pilot scale ball and tower mills, Miner. Eng. 22 (2009) 665–672.

[37] M.G. Melero, J.M. Cano, J. Norniella, F. Pedrayes, M.F. Cabanas, C.H. Rojas, G. Alonso, J.M. Aguado, P. Ardura, Electric motors monitoring: an alternative to increase the efficiency of ball mills, Renew. Energy Power Qual. J. (12) (April 2014).

[38] M.F. Cabanas, M.G. Melero, G. Alonso, J.M. Cano, J. Solares, Maintenance and Diagnostic Techniques for Rotating Electric Machinery, Marcombo Boixareu Editores, Barcelona (Spain), 1999.

[39] B.K. Mishra, R.K. Rajamani, The discrete element method for the simulation of ball mills, Appl. Math. Model. 16 (1992) 598–604.

[40] DEM Solutions, EDEM 2.6 Theory Reference Guide, 2014 (Edinburgh, United Kingdom).

[41] Y. Tsuji, T. Tanaka, T. Ishida, Lagrangian numerical simulation of plug flow of cohesionless particles in a horizontal pipe, Powder Technol. 71 (1992) 239–250.

[42] C.A. Rowland, D.M. Kjos, Rod and ball mills, in: A.L. Mular, R.B. Bhappu (Eds.), Mineral Processing Plant Design, SME, New York, 1980.

[43] M. Rezaeizadeh, M. Fooladi, M.S. Powell, S.H. Mansouri, Experimental observations of lifter parameters and mill operation on power draw and liner impact loading, Miner. Eng. 23 (2010) 1182–1191.

[44] S.H. Kiai, H. Henao, G.-A. Capolino, Analytical and experimental study of gearbox mechanical effect on the induction machine stator current signature, IEEE Trans. Ind. Electron. 45 (4) (Jul–Aug 2009) 1405–1415.

[45] P. Huang, M. Jia, B. Zhong, New method to measure the fill level of the ball mill II — analysis of the vibration signals, Chin. J. Mech. Eng. 24 (4) (2011).